British Journal of Pharmacology (1998) 124, 953–963
http://www.stockton-press.co.uk/bjp

Voltage- and use-dependent inhibition of Na^+ channels in rat sensory neurones by 4030W92, a new antihyperalgesic agent

[1]D.J. Trezise, V.H. John & X.M. Xie

Neurosciences Unit, Glaxo Wellcome Research and Development, Gunnels Wood Road, Stevenage, Hertfordshire SG1 2NY

1 Whole cell patch clamp techniques were used to study the effects of 4030W92 (2,4-diamino-5-(2,3-dichlorophenyl)-6-fluoromethylpyrimidine), a new antihyperalgesic agent, on rat dorsal root ganglion (DRG) neurones.

2 In small diameter, presumably nociceptive DRG neurones under voltage-clamp, 4030W92 (1–100 μM) produced a concentration-related inhibition of slow tetrodotoxin-resistant Na^+ currents (TTX_R). From a holding potential (V_h) of −90 mV, currents evoked by test pulses to 0 mV were inhibited by 4030W92 with a mean IC_{50} value of approximately 103 μM.

3 The inhibitory effect of 4030W92 on TTX_R was both voltage- and use-dependent. Currents evoked from a V_h of −60 mV were inhibited by 4030W92 with a mean IC_{50} value of 22 μM, which was 5 fold less than the value obtained at −90 mV. Repeated activation of TTX_R by a train of depolarizing pulses (5 Hz, 20 ms duration) enhanced the inhibitory effects of 4030W92. These data could be explained by a preferential interaction of the drug with inactivation states of the channel. In support of this hypothesis 4030W92 (30 μM) produced a significant hyperpolarizing shift of 10 mV in the slow inactivation curve for TTX_R and markedly slowed the recovery from channel inactivation.

4 Fast TTX-sensitive Na^+ currents (TTX_S) were also inhibited by 4030W92 in a voltage-dependent manner. The IC_{50} values obtained from V_hs of −90 mV and −70 mV were 37 μM and 5 μM, respectively. 4030W92 (30 μM) produced a 13 mV hyperpolarizing shift in the steady-state inactivation curve of TTX_S.

5 High threshold voltage-gated Ca^{2+} currents were only weakly inhibited by 4030W92. The reduction in peak Ca^{2+} current amplitude produced by 100 μM 4030W92 was 20±6% ($n=6$). Low threshold T-type Ca^{2+} currents were inhibited by 17±8% and 43±3% by concentrations of 4030W92 of 30 μM and 100 μM, respectively ($n=6$).

6 Under current clamp, some cells exhibited broad TTX-resistant action potentials whilst others showed fast TTX-sensitive action potentials in response to a depolarizing current injection. In most cells a long duration (800 ms) supramaximal current injection evoked a train of action potentials. 4030W92 (10–30 μM) had little effect on the first spike in the train but produced a concentration-related inhibition of the later spikes. The number of spikes per train was significantly reduced from 9.7±1.5 to 4.2±1.0 and 2.6±1.1 in the presence of 10 μM and 30 μM 4030W92, respectively ($n=5$).

7 Thus, 4030W92 is a potent voltage- and use-dependent inhibitor of Na^+ channels in sensory neurones. This profile can be explained by a preferential action of the drug on a slow inactivation state of the channel that results in a delayed recovery to the resting state. This state-dependent modulation by 4030W92 of Na^+ channels that are important in sensory neurone function may underlie or contribute to the antihyperalgesic profile of this compound observed *in vivo*.

Keywords: 4030W92; Na^+ channel; dorsal root ganglion; nociceptors; antihyperalgesic

Introduction

Action potential generation and impulse propagation in neurones is triggered by a voltage-activated rise in membrane Na^+ conductance (Hodgkin & Huxley, 1952a,b). This phenomenon is transduced by voltage-gated Na^+ channels, which are a heterogeneous family of membrane proteins derived from many different genes (see Catterall, 1992 for review).

In small diameter, presumably nociceptive sensory neurones of the dorsal root ganglia (DRG) two major Na^+ current phenotypes have been described (Ogata & Tatebayashi, 1992; Roy & Narahashi, 1992; Elliott & Elliott, 1993). One is a rapidly activating and inactivating current which is highly sensitive to the specific Na^+ channel blocker, tetrodotoxin (TTX) and is termed TTX_S. The molecular identity of the channels underlying this current is not clear but mRNA for as many as seven different Na^+ channel α-subunits has been detected in DRG neurones, making it likely that more than one isoform contributes to TTX_S (Waxman *et al*., 1994 Black *et al*., 1996; Black & Waxman, 1996). The second Na^+ current is resistant to block by TTX and has much slower kinetics (TTX_R; see Bossu & Feltz, 1984; Ogata & Tatebayashi, 1992; Roy & Narahashi, 1992; Elliott & Elliott, 1993). An isoform of the voltage-gated Na^+ channel termed 'sensory-neurone specific', or SNS, is believed to underlie TTX_R and the distribution of this protein is restricted to small diameter sensory neurones (Akopian *et al*., 1996; Sangameswaran *et al*., 1996).

Recent experimental evidence has associated and implicated each of these Na^+ currents with chronic pain pathologies of both inflammatory and neuropathic origin. For example, in nociceptive DRG neurones of the rat, hyperalgesic agents such as prostaglandin E_2 and 5-hydroxytryptamine (5-HT) enhance TTX_R and decrease the threshold for channel activation (England *et al*., 1996; Gold *et al*., 1996a; Cardenas *et al*., 1997). Neuronal injury produces dramatic changes in Na^+

[1] Author for correspondence.

channel isoform expression and accumulation of TTX_S. Na^+ channels at the neuroma of lesioned axons are thought to be responsible for the initiation of ectopic discharges (Devor *et al*., 1993; Matzner & Devor, 1994). In each case the neuronal hyperexcitability that results is highly likely to contribute to the induction and maintenance of central sensitization. Thus, voltage-gated Na^+ channels in sensory neurones may provide an attractive target for the development of new analgesic, or antihyperalgesic, agents.

The observation that anaesthetic, anticonvulsant and antiarrhythmic drugs with Na^+ channel blocking properties, can produce analgesia strengthens this supposition. For example, it has been recognized for some time that sub-anaesthetic doses of lignocaine and bupivacaine elevate pain thresholds in man (Boas *et al*., 1982; Back *et al*., 1990; Marchettini *et al*., 1992). In addition, the anticonvulsants phenytoin carbamazepine, and the class 1a antiarrhythmic agent mexiletine are used clinically for the treatment of certain chronic pains of neuropathic origin (Dejgard *et al*., 1988; Tanelian & Brose, 1991; Chabal *et al*., 1992). Early indications suggest that lamotrigine, a novel clinically effective anti-convulsant, is also weakly analgesic (Nakamura-Craig & Follenfant, 1995; Zakrzewska *et al*., 1997).

R(−)-2,4-diamino-5-(2,3-dichlorophenyl)-6-fluoromethyl-pyrimidine (4030W92) is a new chemical entity that is highly effective in experimental models of chronic inflammatory and neuropathic pain (Clayton *et al*., 1998; Collins *et al*., 1998). Interestingly, 4030W92 does not modify nociceptive signalling in the absence of tissue inflammation or nerve injury and exhibits the profile of an 'antihyperalgesic' agent (Clayton *et al*., 1998; Collins *et al*., 1998). To begin to understand the mechanism of action of 4030W92, in the present study we have examined the effects of this agent on voltage-gated Na^+ channels, particularly TTX_R, in sensory neurones of the rat.

Some of the findings of this study have been presented in preliminary form to the British Pharmacological Society (Trezise *et al*., 1998).

Methods

Dissection of dorsal root ganglia

All experiments were performed on dorsal root ganglia (DRGs) isolated from Sprague-Dawley rats of between 3–4 weeks old and of either sex. Rats were killed by decapitation and the whole vertebral column rapidly excises and placed in Ca^{2+}/Mg^{2+}-free Hank's balanced salts solution (HBSS). A 2–3 mm strip of bone was then removed from the dorsal root of the vertebral column to allow bisection of the spinal cord. With the aid of a dissecting microscope, the exposed DRGs in the lumbar, cervical and thoracic regions of each half of the spinal cord were then carefully removed and cleared of adhering connective tissue. Approximately 20–30 ganglia were harvested from each animal.

Dissociation and plating of neurones

Ganglia harvested from one rat were placed in Hams F-12 growth medium supplemented with 10% heat inactivated bovine serum albumin. Enzymatic treatment was performed to soften the ganglia before mechanical dispersal of neurones. Ganglia were first incubated in collagenase (0.125% w/v, 60 min, 37°C), and following 3 washes in serum-free Hams F-12 media, then trypsin (0.025%, 10–15 min, 37°C). After the second incubation period, ganglia were washed 5 times with serum-containing media to inactivate the trypsin. In 0.5 ml final volume, neuronal dispersal was carried out by gently triturating the ganglia with a series of progressively finer diameter plastic, portex cannulae. Trituration was terminated as soon as a cloudy suspension of cells appeared in the media. Neurones were plated onto glass coverslips, previously treated with poly-DL-ornithine (0.5 mg ml^{-1} overnight) and laminin (10 $\mu g\ ml^{-1}$, 15 min), and maintained in serum-containing media at 37°C in a humidified atmosphere of 95% air : 5% CO_2.

Electrophysiological recording

Electrophysiological experiments were conducted on neurones of 10–25 μm somatic diameter within 1–36 h of plating. All experiments were performed at room temperature (20–22°C). The contents of the external (bath) and internal (pipette) solutions are shown in Table 1. Drugs were applied either via addition to the bath perfusate or using a rapid perfusion system which consisted of a series of reservoirs connected to a small microfil tube which was placed 400–600 μm from the cell. Whole-cell currents were recorded using an Axopatch 200B amplifier (Axon Instruments; Hamill *et al*., 1981). Patch pipettes were fabricated from 1.5 mm outside diameter borosilicate capillary glass (Clark Electromedical) using a micropipette puller (Sutter model P97), and fire polished (Narishige Microforge) to give final tip resistances of 2–4 mΩ. A silver/silver chloride pellet was used as the bath reference electrode and the potential difference between this and the recording electrode was adjusted for zero current flow before

Table 1 Constituents of internal recording solutions and external bath perfusate

NA^+ currents				*Ca^{2+} currents*				*Membrane potential (under current clamp)*			
Internal		*External*		*Internal*		*External*		*Internal*		*External*	
110	CsF	60	NaCl	105	CsCl	10	$CaCl_2$	140	KCl	130	NaCl
10	HEPES	10	HEPES-Na	40	HEPES	5	HEPES	10	HEPES	10	HEPES
5	$MgCl_2$	5	$MgCl_2$	2.5	$MgCl_2$	100	ChCl	2	$MgCl_2$	2	$MgCl_2$
10	NaCl	5	KCl	5	D-Glucose	30	TEACl	11	EGTA	3	KCl
		50	ChCl	3	Mg-ATP	0.001	TTX	2	Mg-ATP	1.2	$NaHCO_3$
		1	$CaCl_2$	0.5	Li-GTP			0.5	Li-GTP	10	Glucose
		0.2	$CdCl_2$	14	Phosphocreatine						
				50*	Creatine phosphokinase						

Values shown are final mM concentrations, with the exception of the creatine phosphokinase which is expressed in *units ml^{-1}. All solutions were made up in distilled water. Internal solutions were adjusted where necessary to a final pH of 7.25 and osmolarity of 285–290 mOsmol and filtered. External solutions were adjusted to PH 7.4 and osmolarity 295–300 mOsmol. TTX-resistant Na^+ currents were recorded in the presence of TTX (0.5 μM).

seal formation. Cells were visualized using a Diaphot200 inverted microscope (Nikon) with modulation contrast optics at a final magnification of ×400. The somatic diameter of neurones was measured using an eyepiece micrometer. High resistance seals (1–10GΩ) between pipette and neuronal cell membranes were achieved by gentle suction, and the 'whole cell' configuration attained by applying further suction.

Voltage command protocols were generated, and current records stored, via a digidata1200 analogue/digital interface (Axon Instruments) controlled by microcomputer (Viglen Pentium) using pCLAMP6 Clampex software (Axon Instruments). Signals were prefiltered at 5 kHz bandwidth and sampled at 20 kHz. Capacitance transients and series resistance errors were compensated for (80–85%) using the amplifier circuitry, and linear leakage currents were subtracted using an on-line 'P-4' procedure provided by the commercial software package. In most cases evoked Na^+ currents ranged from −600pA to −4500pA and thus the maximum estimated voltage drop across the compensated series resistance amounted to less than 4 mV. Liquid junction potentials occurring subsequent to seal formation (2–6 mV) were not corrected for. Digitized data files were stored on the microcomputer hard drive for offline analysis.

Analysis of data

Data were analysed using pCLAMP6 (Clampfit), ORIGIN and DAISI data handling and graphical presentation software packages. Results are presented as either arithmetic mean ± s.e.mean or geometric mean with 95% confidence limits, where appropriate; *n* refers to the number of cells in each experimental group, which were obtained from at least 2 different animals in all cases. Statistical comparisons were made using paired or unpaired Student's *t* test and considered of significance when $P<0.05$.

For construction of activation curves, Na^+ conductance (g_{Na}) was calculated from the peak current (I_{Na}), according to the following equation: $g_{Na}=I_{Na}/V\text{-}E_{Na}$ where V is the test pulse potential and E_{Na} the membrane potential at which the peak current is reversed. Normalized Na^+ conductance was plotted against test pulse potentials and fitted to a Boltzman function according to the equation; $g/g_{Max}=1/[1+\exp(V_{1/2}-V/k)$ where g is the measured conductance, g_{Max} is the maximal conductance, $V_{1/2}$ is the membrane potential at which the half-maximal channel open probability occurs and k is the slope of the curve. For construction of inactivation curves, the peak current (I) was normalized relative to the maximal value (I_{Max}) obtained at a holding potential (V_h) of −90 mV and plotted against the conditioning pulse potential. Data were fitted by a Boltzman function according to the following equation: $I/I_{Max}=1/[1+\exp(V_{1/2}-V/k)$ where V is the membrane potential during prepulses, $V_{1/2}$ the potential at which the half-maximal channel inactivation occurs and k the slope of the line.

For fitting drug concentration-response curves, an independent binding site model of the form; $I=a-d/1+(\times/IC_{50})^b)+d$ was used, where I is the current in the presence of drug, a the normalized peak current before drug, b the Hill slop value, d the maximum inhibitory effect, × the drug concentration and IC_{50} the drug concentration required to produce 50% current inhibition. To assess current kinetics, time constant (τ) values defined as the time to achieve 50% current activation (τ_{act}) and 50% inactivation (τ_{inact}) were obtained by fitting the respective phases of the current traces to single exponential functions of the order; $A\times\exp[-t/\tau]+C$ where A is the current amplitude at the start of the fitting region, t the time and C the steady-state asymptote. Best fits were obtained using the Chebyshev transformation non-iterative curve fitting technique.

Drugs and solutions

The following drugs and solutions were used in this study; sodium chloride (NaCl), potassium chloride (KCl), choline chloride, magnesium chloride heptahydrate ($MgCl_2$), N-(2-hydroxyethyl)piperazine-N′-(2-ethanesulphonic acid) (HEPES), HEPES-Na, laminin, tetrodotoxin, poly-DL-ornithine hydrobromide (all Sigma), ethylene glycol-bis(β-aminoethyl ether) N,N,N′,N′-tetraacetic acid (EGTA; Fluka Biochemika), calcium chloride ($CaCl_2$; BDH Chemicals), tetraethylammonium chloride (TEA), caesium fluoride (CsF; Aldrich Chemical Co.), collagenase type III (130 units mg^{-1}), trypsin TPCK (226 units mg^{-1}; Worthington Biochemical corporation), **R**(−)-2,4-diamino-5-(2,3-dichlorophenyl)-6-fluoromethylpyrimidine (4030W92; Medicinal Sciences Unit, Glaxo-Wellcome, Stevenage, U.K.). All drugs and chemicals were dissolved in distilled water (or cell culture media where appropriate), with the exception of 4030W92 for which 10% 1 N HCl was the solvent. Hank's balanced salt solution (HBSS) comprised (mM in double distilled water); NaCl 137, KCl 5, Na_2HPO_4 0.4, KH_2PO_4 0.5, $NaHCO_3$ 4.2 and glucose 5.6, pH 7.3.

Results

Voltage-gated Na^+ currents

Voltage-gated Na^+ currents ranged from 200 pA to >10 nA peak amplitude under the conditions of reduced extracellular Na^+ concentration. Generally the voltage control of cells with Na^+ currents exceeding 6 nA was inadequate and these cells were rejected. Currents tended to increase in amplitude during the first 15 min after achieving the whole cell recording configuration. All drug manipulations were performed after this period and during which currents were very stable (15–90 min). On the basis of kinetics of activation and inactivation, and sensitivity to TTX (500 nM), two clear current phenotypes could be identified: (1) rapidly activating and inactivating TTX-sensitive Na^+ current (TTX_S) and (2) TTX-resistant Na^+ current with slow kinetics (TTX_R). In a proportion of neurones both types of current were observed and could be readily separated using TTX (500 nM; see Ogata & Tatebayashi, 1992; Roy & Narahashi, 1992; Elliott & Elliott, 1993). All studies on TTX_R were recorded in the presence of 500 nM TTX.

Effect of 4030W92 on TTX_R Na^+ currents

4030W92 (1–300 μM) reduced the amplitude of the peak TTX_R current (V_h −90 mV, V_{test} 0 mV) in a concentration-dependent manner (Figure 1). From a V_h of −90 mV, the mean IC_{50} value for this effect was 103 μM (68–155 μM, 95% confidence interval values for the line of best fit; $n=5$–11). The inhibitory effect of 4030W92 was voltage-dependent in that a significantly lower IC_{50} value was obtained when Na^+ currents were evoked from a V_h of −60 mV (mean IC_{50} value 22 μM (13–38 μM); $n=5$–11; $P<0.05$ *vs* V_h −90 mV). Upon washout, complete reversal of the effect of 4030W92 could generally be achieved with low drug concentrations (<10 μM), whilst at higher concentrations, only partial reversal was observed.

Use-dependent actions of 4030W92 at different pulse widths were evaluated with trains of repeated voltage steps to 0 mV

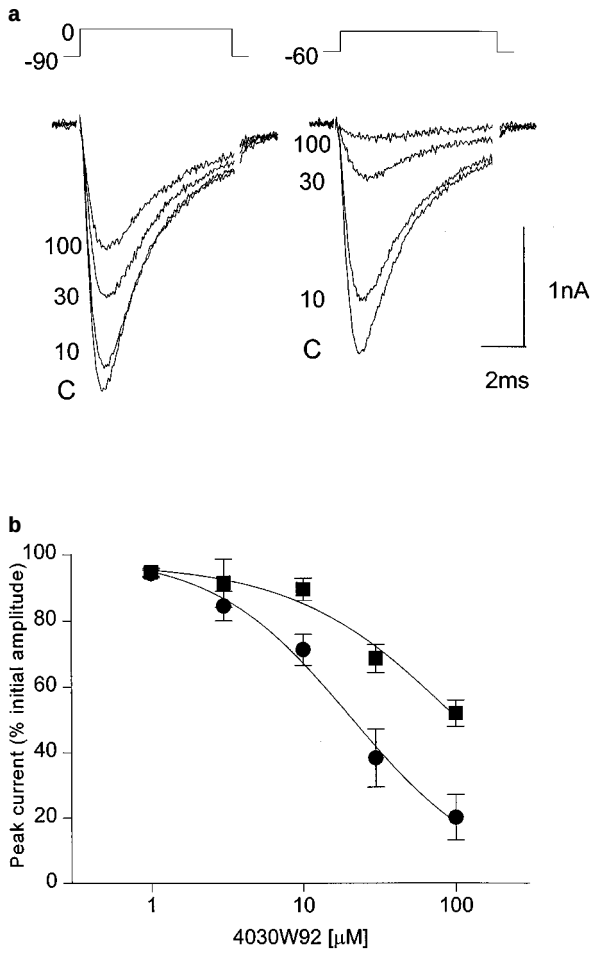

Figure 1 Voltage-dependent inhibition of TTX-resistant Na^+ currents by 4030W92 in rat sensory neurones. Neurones were voltage-clamped at either −90 mV or −60 mV and stepped to the test potential (0 mV) for 10 ms. (a) A representative experiment from a single neurone where currents in the absence and presence of increasing concentrations of 4030W92 have been superimposed. Residual capacitance transients have been blanked for clarity. Note the much more marked inhibitory effect of the drug at a V_h of −60 mV compared to −90 mV. (b) The concentration-effect curve for this inhibition. The abscissa scale represents the micromolar concentration of 4030W92 and the ordinate scale the peak current expressed as a percentage of the current obtained in the absence of drug. Data were fitted to an independent binding site model and yielded IC_{50} and Hill slope values of 22 μM and 1.02, respectively for V_h −60 mV (solid circle) and 103 μM and 0.78 for V_h −90 mV (solid square). Each point represents the mean value and the vertical lines the s.e.mean (n=5–11).

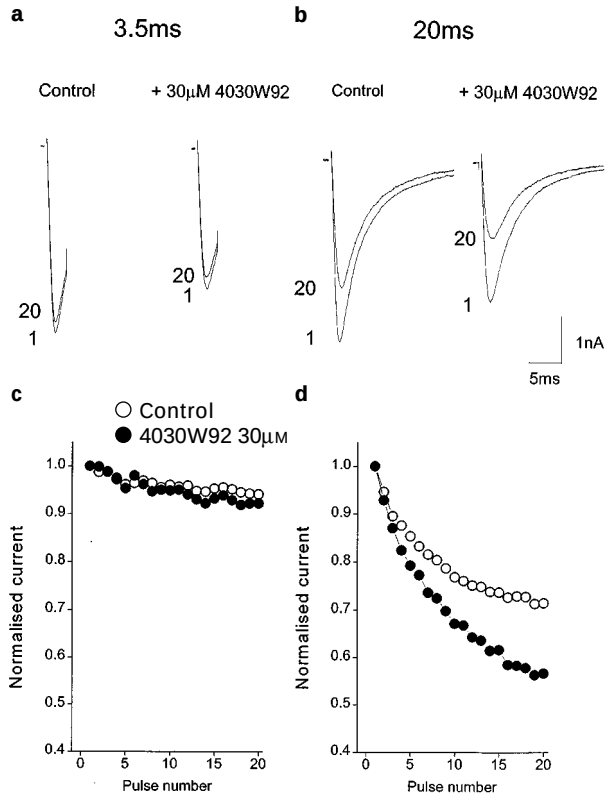

Figure 2 Use-dependent inhibition by 4030W92 of TTX-resistant Na^+ channels in rat sensory neurones. Na^+ currents evoked by trains of depolarizing pulses (V_h −90 mV, V_{test} 0 mV, 5 Hz) of either 3.5 ms (a) or 20 ms (b) duration were recorded in the absence (control) and the presence of 30 μM 4030W92. Superimposed records of currents obtained from the 1st and the 20th pulse in a train are displayed. In the example shown the ratios of the amplitudes of the 20th to the 1st pulse were 94% and 71% for the 3.5 ms and 20 ms controls, respectively, and 92% and 56% in the presence of 4030W92. In the lower panels the current amplitude, normalized with respect to the 1st pulse, is plotted against the pulse number. Note the greater inhibition of 4030W92 upon repeated current activation ('use-dependence') with the longer pulses in (d) compared to the shorter pulses in (c).

from a V_h of −90 mV. With very short duration pulses (3.5 ms) delivered at 5 Hz, there was little decay in the peak amplitude of evoked currents. The ratio of the 20th to the 1st pulse was 0.97±0.01 (n=4). In the presence of 30 μM 4030W92 no significant use-dependent drug action was observed at this pulse width (0.94±0.02; n=4, P>0.05 paired Student's t test). In contrast, 4030W92 (30 μM) produced a significant use-dependent effect on pulses of longer duration (20 ms, 5 Hz); control 0.73±0.18, drug 0.61±0.16 (n=4; Figure 2).

Current-voltage (I-V) relationships for TTX_R were determined in the absence and presence of 4030W92 using a series of depolarizing steps from a V_h of −90 mV. The peak current amplitude was signficantly reduced to 85.8±0.1% and 74.4±0.1% of the pre-drug value by 10 and 30 μM 4030W92, respectively (n=4). However, there was no significant change in either the shape of the I-V curve, the pulse potential at which the peak current was observed (0 mV) or the current reversal potential (Figure 3). When membrane Na^+ conductance was calculated, it was clear that 4030W92 did not significantly shift the voltage range across which channel activation occurred. The control mean half-maximal voltage ($V_{1/2}$) for activation and slope (k) value of the curve were respectively −16±3 mV and 6.5±1.1 in the absence of drug, −16±4 mV and 6.2±1.1 in the presence of 10 μM 4030W92, and −18±5 mV and 6.0±0.9 in the presence of 30 μM 4030W92 (n=4; NS, Figure 3).

The rates of both activation and inactivation of TTX_R were voltage-dependent, and for any given test pulse potential, each time course could be well fitted by a single exponential. Current activation generally proceeded between 5–6 times more rapidly than inactivation. Neither 10 μM nor 30 μM 4030W92 had any significant effect on the kinetics of activation and inactivation of TTX_R. The mean τ_{act} and τ_{inact} values for a test pulse to 0 mV from a V_h of −90 mV were, respectively, 0.5±0.1 ms and 3.4±0.4 ms in the absence of drug, 0.5±0.002 ms and 3.3±0.3 ms in the presence of 10 μM 4030W92, and 0.5±0.01 ms and 3.2±0.2 ms in the presence of 30 μM 4030W92 (NS; n=4).

Voltage-dependence of 'fast' and 'slow' channel inactivation was studied using standard two pulse protocols from a V_h of

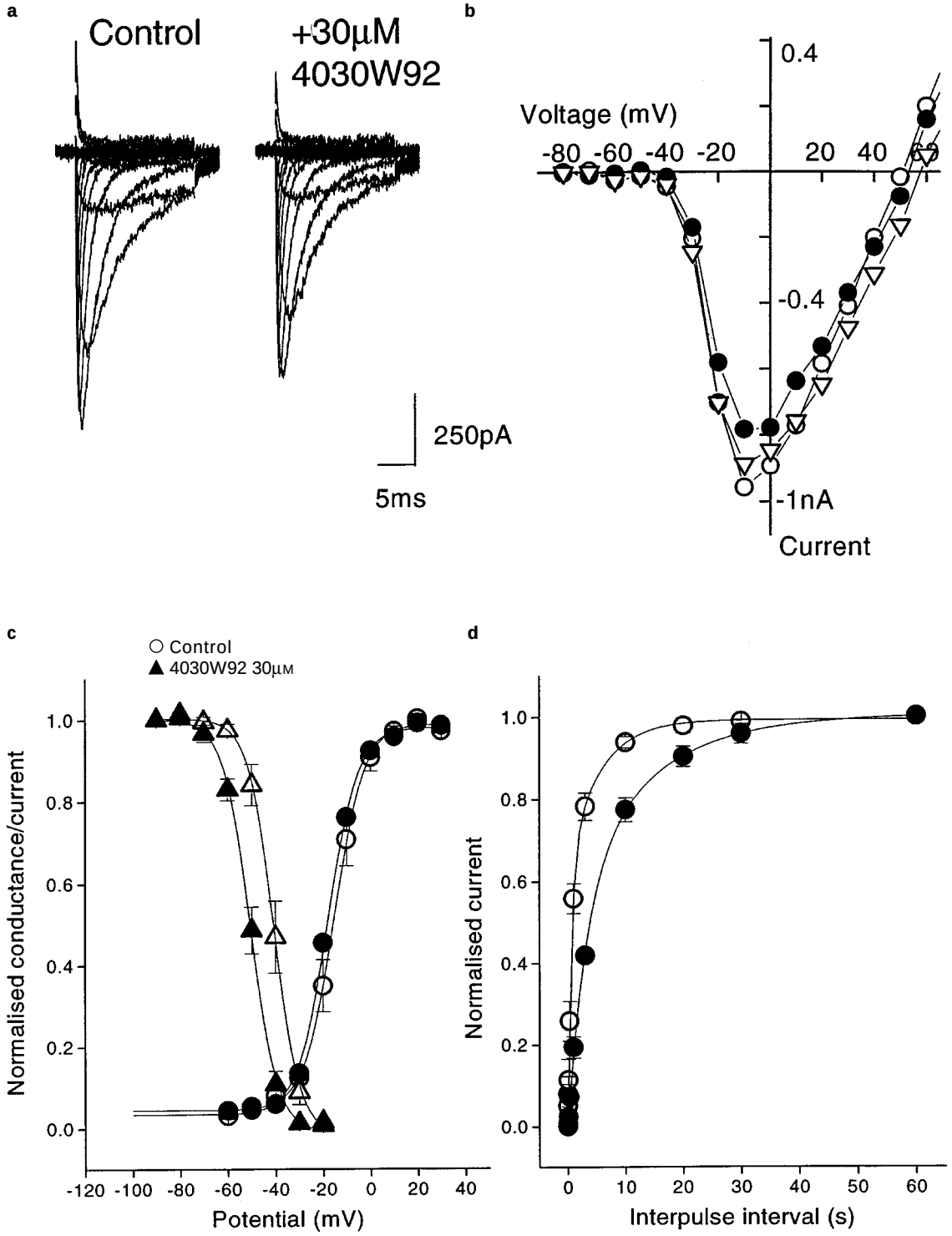

Figure 3 Effect of 4030W92 on TTX_R Na^+ current-voltage (*I*-V) relationship (a and b), conductance and steady state-inactivation (c), and recovery from inactivation (d). In each panel control values are represented by the open symbols and values obtained in the presence of 30 μM 4030W92 by the solid symbols. All experiments were conducted from a V_h of -90 mV. Representative records of *I*-V relationships in the absence and presence of 30 μM 4030W92 are shown in (a) and the peak currents evoked at each potential are plotted in (b). Responses after washout of 4030W92 are represented by open triangles. In (c) the abscissa scale represents the pulse potential and the ordinate scale either normalized conductance or current. For conductance, the lines of best fit represent Boltzmann functions with $V_{1/2}$ values of -15 mV and -18 mV, and slope parameters of 6.29 and 6.33 in the absence control and presence of drug, respectively. The steady-state inactivation curves were constructed using 4 s conditioning pulses to different potentials followed immediately by the test pulse to 0 mV. Lines of best fit represent Boltzmann functions with $V_{1/2}$ values of -40 mV and -51 mV, and slope parameters of 5.33 and 5.38. In (d) the recovery from inactivation was determined using a two pulse protocol with a 4 s conditioning pulse, a varying interpulse interval and then a second pulse to 0 mV. The lines of best fit are double exponential functions with τ values of 0.67 s (A1 0.35) and 5.44 s (A2 0.62) in control, and 3.23 s (A1 0.55) and 13.26 s (0.45) in the presence of 4030W92. In (c) and (d), points represent the mean values and vertical lines the s.e.mean ($n=4-6$).

−90 mV. To study 'fast' inactivation, conditioning pulses of 15 ms to varying potentials of between −80 and +70 mV were delivered, followed by a test pulse to 0 mV to evoke the residual (non-inactivated) current. Using this protocol, the control $V_{1/2}$ and k values for inactivation were -19 ± 2 mV and 6.9 ± 0.4, respectively ($n=7$). In the presence of 4030W92 (30 μM) a small, but significant, leftward displacement of the normalized inactivation curve ($V_{1/2}=-24\pm1$ mV) and a reduction in the slope parameter ($k=8.0\pm0.4$; $n=4$; both $P<0.05$ compared to control, Student's paired t test) was observed. Slow inactivation was studied using 4 s conditioning pulses, and occurred at much more hyperpolarized potentials (-40 ± 2 mV and 4.7 ± 0.1 ($n=5$)). In the presence of 4030W92 (30 μM) this inactivation curve was significantly displaced to the left (Figure 3), such that $V_{1/2}$ and k values of -50 ± 1 mV and 5.4 ± 0.1 were obtained ($n=5$; $P<0.05$, Student's paired t test).

Two-pulse protocols with varying interpulse intervals were employed to evaluate the effect of 4030W92 on the rate of recovery from channel inactivation. With short conditioning pulses of 20 ms duration from a V_h of −90 mV to 0 mV (V_{con}) recovery from channel inactivation (fast) occurred extremely rapidly. The time course of this recovery could be best fitted by the sum of two exponentials with mean τ values of 1.1 ± 0.2 ms (τ_1) and 132 ± 16 ms (τ_2, $n=4$). In the presence of 4030W92 (30 μM) there was a delay in the rate of recovery from fast inactivation ($\tau_1=2.4\pm0.3$ and $\tau_2=89\pm7$ ms, respectively ($n=4$)). If much longer conditioning pulses were used (4 s, V_h −90 mV, V_{con} −30 mV) in order to generate slow inactivation, recovery occurred much more slowly ($\tau_1=$ 674 ms, $\tau_2=5452$ ms). 4030W92 (30 μM) substantially delayed recovery from these longer depolarizations ($\tau_1=3329$ ms, $\tau_2=13275$ ms; Figure 3; $P<0.01$).

Effect of 4030W92 on TTX_S Na^+ currents

4030W92 (3–100 μM) also inhibited TTX_S Na^+ currents in rat DRG neurones (Figure 4). The mean IC_{50} value for currents evoked from a V_h of −90 mV (V_{test} 0 mV) was 37 μM (22–61 μM) with a Hill slope of 0.81 ($n=4$). The inhibition of TTX_S was voltage-dependent as evidenced by the significantly lower IC_{50} value obtained from a V_h of −70 mV (5 μM (4–9 μM), slope 0.62, $n=5$; $P<0.05$). As was the case with TTX_R, 4030W92 produced a significant hyperpolarizing shift in the slow inactivation curve for TTX_S (1 s conditioning pulse). The control $V_{1/2}$ and k parameters were -76 ± 5 mV and 7.6 ± 0.8, respectively, compared to values of -88 ± 7 mV and 9.1 ± 0.7 in the presence of 30 μM 4030W92 ($n=5$, $P<0.05$, paired Student's t test).

Effect of 4030W92 on voltage-gated Ca^{2+} currents

Ca^{2+} currents were recorded from a total of 8 neurones. Current-voltage relationships were constructed with a series of depolarizing steps (60 ms duration, 0.5 Hz) from −50 mV to +40 mV from a V_h of −60 mV. With this protocol and under the recording conditions there was no evidence of current rundown. In 6 out of 8 neurones both low threshold, transient T-type currents (mean amplitude 213 pA, range 79–410 pA) and high threshold slowly inactivating currents were observed (mean amplitude 905 pA, range 529–1347 pA). In the remaining 2 cells only a high threshold current was present. All active currents were inhibited by 200 μM Cd^{2+} (data not shown).

4030W92 exerted only weak inhibition of high threshold Ca^{2+} currents (V_h −60 mV, V_{test} +20 mV). With 30 μM and 100 μM 4030W92 the mean reduction in current amplitude was $8\pm3\%$ ($n=5$) and $20\pm3\%$ ($n=8$), respectively. T-type Ca^{2+} currents (V_h −60 mV, V_{test} −30 mV) were significantly more sensitive to 4030W92; the mean reduction in current amplitude at concentrations of 30 μM and 100 μM 4030W92 was $17\pm6\%$ ($n=3$) and $43\pm8\%$ ($n=6$), respectively (each $P<0.05$ compared to high threshold current inhibition). The effects of 4030W92 on Ca^{2+} currents are summarized in Figure 5.

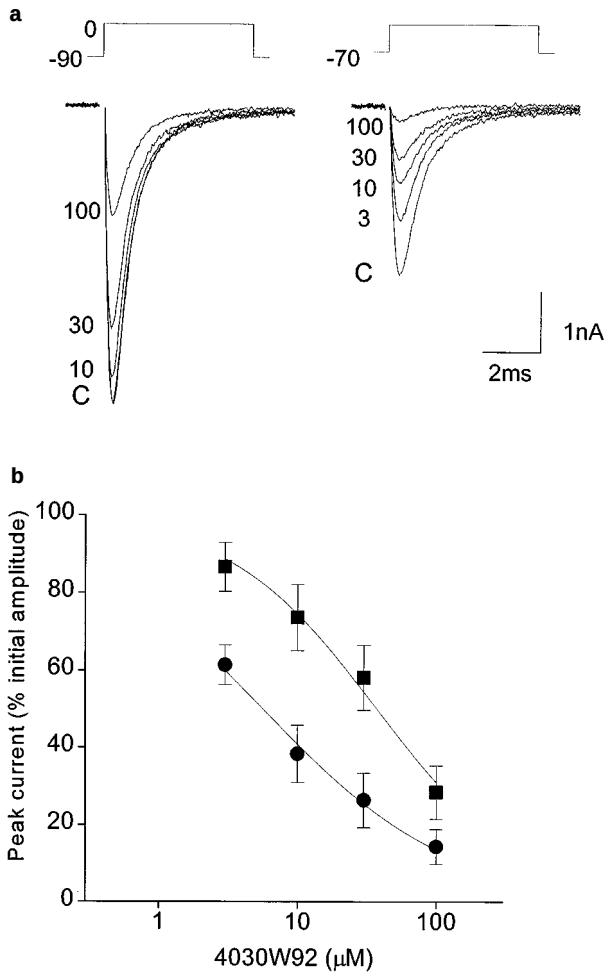

Figure 4 Voltage-dependent inhibition of TTX-sensitive Na^+ currents by 4030W92 in rat sensory neurones. Neurones were voltage-clamped at either −90 mV or −70 mV and stepped to the test potential (0 mV) for 10 ms. (a) A representative experiment from a single neurone where currents in the absence and presence of increasing concentrations of 4030W92 have been superimposed. Note the much more marked inhibitory effect of the drug at a V_h of −70 mV compared to −90 mV. (b) The concentration-effect curve for this inhibition. The abscissa scale represents the micromolar concentration of 4030W92 and the ordinate scale the peak current expressed as a percentage of the current obtained in the absence of drug. Data were fitted to an independent binding site model and yielded IC_{50} and Hill slope values of 37 μM and 0.81, respectively for V_h −90 mV (circles) and 5 μM and 0.62 for V_h −70 mV (squares). Each point represents the mean value and the vertical lines the s.e.mean ($n=5$).

Effect of 4030W92 on trains of action potentials

Current clamp recordings were made from 23 neurones. Generally, cell resting membrane potentials were stable and quiescent and only the occasional spontaneous action potential was observed (<0.1 Hz). Resting membrane potentials ranged from −43 to −64 mV (mean value -56 ± 1 mV; $n=12$), and

input resistances, as determined with small hyperpolarizing current pulses (−0.05 nA, 100 ms), ranged from 80 to 300 MΩ.

Supramaximal current injection intensities for evoking action potentials were determined using short depolarizing (3–10 ms) pulses (0.05 to 0.6 nA). Between neurones a variety of action potential shapes were encountered, ranging from rapidly rising and repolarizing spikes with action potential widths of <3 ms (measured at 50% of the peak height) to broad TTX-resistant action potentials with a clear inflexion on the repolarizing phase (spike width 4–8 ms; see Caffrey *et al*., 1992; Cardenas *et al*., 1995). In 4 neurones with action potentials less than 3 ms duration TTX (100 nM) abolished the spike evoked by current injection, whilst in 4 neurones with broad action potentials (>4 ms) and inflected repolarization phases TTX (100 nM) had little or no effect.

4030W92 (10–30 μM) had no significant effects on cell resting membrane potential (control; −60.8±2.2 mV, 10 μM −61.3±2.5 mV 30 mM −59.2±1.6 mV; $n=7$; NS). The amplitude of a single evoked action potential, defined as the difference between resting membrane potential and the peak of the spike, was slightly reduced from 105±3 mV to 97±2 mV and 90±3 mV in the presence of 10 and 30 μM 4030W92, respectively ($P<0.05$ *vs* control). This effect was reversed on washout (103±3 mV; $n=5$). There was also a small increase in the spike width in the presence of 4030W92 (control, 3.0±0.6 ms, 10 μM 3.6±0.6 ms, 30 μM 4.6±0.6 ms, wash 3.1±0.6 ms ($n=5$)). The latency to the spike, defined as the time from the start of the current injection period to the peak of the spike was also slightly increased (control 14±4 ms, 10 μM 15±4 ms, 30 μM 17±5 ms, wash 13±3 ms, $n=5$).

Longer durations of supramaximal depolarizing current injection (400–800 ms) produced a train of action potentials in 19 out of 23 cells. In the remaining 4 cells only a single spike was observed irrespective of how much current was injected into the cell. In the neurones that fired trains of spikes it was not always possible to obtain reproducible responses to constant current injection. However, in 5 cells very reproducible responses were observed. Of these, 2 out of 5 had action potential widths of less than 2 ms, another 2 had broad, inflected action potentials (4–5 ms) and the final cell was in between (spike width 2.5 ms). In all 5 cells 4030W92 (10–30 μM) produced a similar, reversible effect which was to reduce the total number of action potentials by preferentially

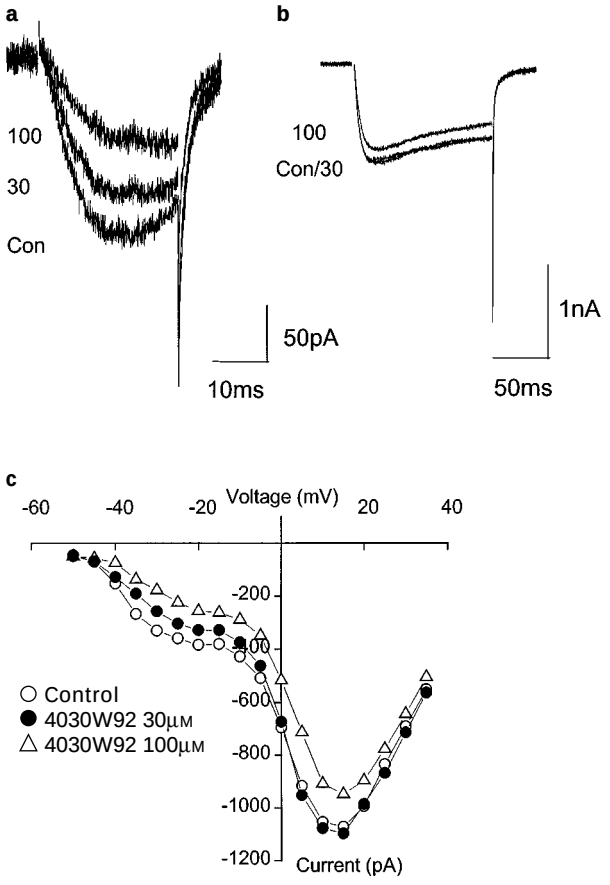

Figure 5 Effect of 4030W92 on votage-gated Ca^{2+} currents in rat dorsal root ganglion neurones. (a) Representative records of low threshold 'T'-type Ca^{2+} currents evoked by depolarizing pulses from a V_h of −60 mV to −30 mV, in the absence (denoted by Con) and the presence of 30 and 100 μM 4030W92. (b) The smaller inhibitory effect of 4030W92 on high threshold Ca^{2+} current (V_h −60 mV, V_{test} +15 mV) in the same neurone. The current-voltage relationship in the absence and presence of drug is shown in (c). The ordinate scale represents the peak current amplitude (pA) and the abscissa scale the test pulse potential (mV).

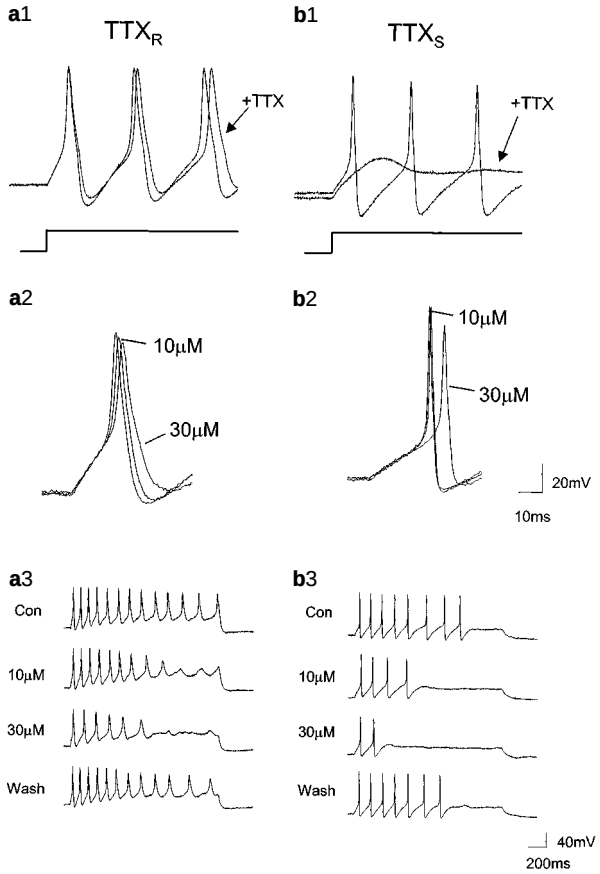

Figure 6 Modulation by 4030W92 (10–30 μM) of action potential firing in isolated rat dorsal root ganglion neurones under current-clamp conditions. Representative membrane potential records from a TTX-resistant neurone are shown on the left hand side (a1-3) and from a TTX-sensitive neurone on the right hand side (b1-3). (a) Superimposed action potentials in response to current injection in the absence and presence of 100 nM TTX. Note the broad action potential with the inflexion on the repolarization phase of the TTX-resistant cell. In (a3) and (b3) trains of spikes in response to supramaximal current injection stimulus (800 ms duration) are shown in control, in the presence of 10 μM and 30 μM 4030W92 and after washout. Note the marked, concentration-related spike adaptation in the presence of 4030W92 in both cells. (a2) and (b2) The early phase of the records in (a3) and (b3) superimposed; 4030W92 had only a small inhibitory effect on the initial spike.

inhibiting the later spikes in the train. When grouped together, the mean number of spikes during an 800 ms current injection period was 9.7 ± 1.5 under control conditions and 4.2 ± 1.0 and 2.6 ± 1.1, in the presence of 10 and 30 μM 4030W92, respectively. After washout of the drug, the mean number of spikes recovered to 7.8 ± 1.3 ($n = 5$; Figure 6).

In 2 cells it proved possible to study the frequency-dependence of drug action by evoking trains of action potentials with different current injection intensities. In both cells 4030W92 (10 μM) clearly had little effect on resting membrane potential, the properties of a single spike or even when 2–4 action potentials were evoked. However, when longer trains of action potentials were evoked 4030W92 (10 μM) markedly enhanced spike adaptation. The relationship between current injection intensity and excitatory response in the absence and presence of 4030W92 is shown in Figure 7.

Discussion

The present study describes electrophysiological experiments on 4030W92, a new antihyperalgesic agent (Clayton *et al*., 1998; Collins *et al*., 1998), in small diameter presumably nociceptive sensory neurones of the rat.

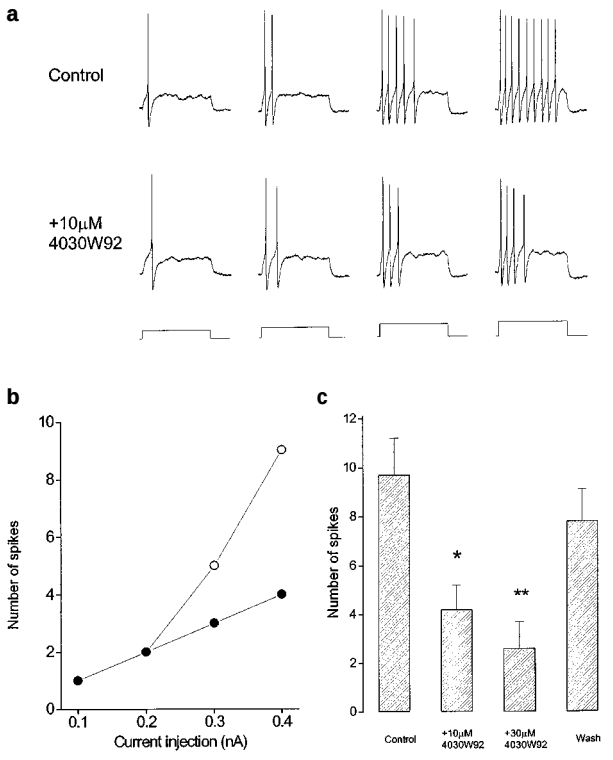

Figure 7 Frequency-dependent inhibition of action potential firing in rat sensory neurones by 4030W92. In (a) responses to increasing current injection intensities (0.1–0.4 nA, 400 ms) are shown in the absence (upper panel) and presence (lower panel) of 10 μM 4030W92. The number of evoked spikes is plotted against current injection intensity in (b) (open circles, solid circles, 10 μM 4030W92). Note the lack of effect of 4030W92 on 1–2 evoked spikes but the abbreviation of the longer trains of action potentials evoked by higher current injection intensities. (c) A histogram of the mean number of spikes ($\pm$s.e.mean) obtained in 5 neurones following supramaximal current injection (800 ms). In each neurone the number of spikes per train (averaged from 3 consecutive trains) was determined under control conditions, in the presence of 10 and 30 μM 4030W92, and after washout. Statistically significant reductions in the number of spikes per train are denoted by $^*P < 0.05$ and $^{**}P < 0.01$; paired Student's t test.

4030W92 inhibited tetrodotoxin-resistant Na^+ currents (TTX_R) in a state-dependent manner. When channels were opened by depolarization from a negative holding potential (−90 mV), at which little or no steady state channel inactivation occurs, 4030W92 produced only weak inhibition. Under these conditions the IC_{50} value of 103 μM represents a good estimation of the drug affinity for the resting (non-inactivated) channel state. Importantly, the inhibition of TTX_R by 4030W92 was enhanced when the membrane was held at relatively positive potentials, as judged by the significantly lower IC_{50} value of 22 μM that was obtained from a V_h of −60 mV. It might be anticipated that the potency of 4030W92 would be further increased at potentials more positive than −60 mV. Our efforts to demonstrate this point were hampered by the spontaneous decline in the absence of the drug of the amplitude of currents evoked from more depolarized potentials. Nevertheless, a significant voltage-dependent action of the drug was clearly evident.

The most likely explanation for this phenomenon is that 4030W92 preferentially interacts with a channel inactivation state of TTX_R. Under depolarization conditions enhanced drug actions are predicted since a considerable proportion of channels are inactivated and thus susceptible to drug modulation/binding. The observation that 4030W92 produced a hyperpolarizing shift in the voltage-dependence of inactivation curve and slowed recovery from channel inactivation supports this contention. Interestingly, the effects of 4030W92 were more pronounced when long conditioning pulses were employed, suggesting that the drug interacts preferentially with a slow inactivation state. The affinity for the slow inactivated state can be estimated at 3 μM using the equation, $K_i = L/[1 + L/K_c/\exp(\Delta V_{1/2}/k) - 1]$, where L is the drug concentration, K_c is the apparent dissociation constant for the resting state, $\Delta V_{1/2}$ the shift in the half-inactivation voltage produced by the drug and k is the slope of the inactivation curve in the absence of drug. This represents a selectivity of 30 fold for inactivated compared to resting TTX_R Na^+ channels.

4030W92 also produced voltage-dependent inhibition of TTX-sensitive Na^+ currents in rat DRG neurones. Indeed the IC_{50} estimate for inhibition of currents evoked from a V_h of −90 mV was some 3 fold lower than for TTX_R, suggesting that 4030W92 may have some selectivity for TTX_S. However, it should be noted that the steady-state inactivation curve for TTX_S is some 20 mV more negative than TTX_R, and thus at any given membrane potential more TTX_S than TTX_R Na^+ channels will be inactivated. At potentials across which inactivation occurs, therefore, preferential binding of 4030W92 to inactivated states will favour inhibition of TTX_S over TTX_R (see also Song *et al*., 1996; 1997; Rush & Elliott, 1997). However, a much higher proportion of TTX_S channels will already be inactivated at or around the resting membrane potential (−50 to −65 mV) and so would not be available for gating even in the absence of drug. Thus, in neurones in which both TTX_S and TTX_R channels are present the net effect on Na^+ conductance will be a combination of the different sensitivites of each channel with their available current densities.

The use-dependent inhibition of TTX_R by 4030W92 can also be rationalized in terms of preferential binding of 4030W92 to inactivated states. With repeated short pulses of 3.5 ms duration, little rundown of current was obtained both in the absence and presence of drug. Such pulses are of insufficient length to generate significant channel inactivation and thus no extra drug effect over the above the tonic inhibition would be anticipated. Increasing pulse duration to 20 ms generates inactivation that accumulates when test pulses

are repeated at a frequency of 5 Hz. Under these conditions, 4030W92 (30 μM) produced a significant use-dependent effect. With these longer pulses a significant fraction of channels is converted into the slow inactivated state and thus become susceptible to drug binding/modulation. The interaction of 4030W92 with this channel state that results in delayed recovery is manifest as an enhanced inhibition on repeated channel gating ('use-dependence').

Thus, the votage-clamp data indicate that 4030W92 selectively interacts with the slow inactivated state of Na^+ channels in sensory neurones to yield voltage- and use-dependent inhibitory effects. A similar state-dependent modulation of brain Na^+ and cardiac channels was observed with certain anticonvulsant, neuroprotective, local anaesthetic and anti-arrhythmic drugs (e.g. phenytoin, carbamazepine, riluzole, 619C89, lidocaine and mexiletine) (Ragsdale *et al*., 1991; Sunami *et al*., 1993; Herbert *et al*., 1994; Kuo & Bean, 1994; Xie & Garthwaite, 1996). However, there are few detailed studies on the effects of these other drugs on Na^+ channels, especially TTX_R, and on action potential firing patterns in DRG neurones for direct comparison with the actions of 4030W92. The available data suggest that phenytoin and carbamazepine are only weak inhibitors of TTX_R and exhibit a low degree of voltage-dependence (Song *et al*., 1996; Rush & Elliott, 1997) whilst riluzole, unlike 4030W92, shifts the voltage-dependence of activation and accelerates inactivation of TTX_R (Song *et al*., 1997). Tonic and use-dependent inhibitory effects of lidocaine on TTX_R have been documented (Roy & Narahashi, 1992), but there are no reports to our knowledge of the effects of mexiletine on this current. It would be interesting to compare directly the profile of action of 4030W92 with other agents which possess Na^+ channel inhibitory properties to determine similarities and differences in cellular mechanisms of action, which might be relevant to the use and potential of these agents in clinical pain management.

High threshold voltage-gated Ca^{2+} currents, evoked from around the resting membrane potential (-60 mV), were only weakly inhibited by 4030W92. Previous workers have shown that the high threshold Ca^{2+} current in rat sensory neurones is comprised of N-type, neuronal L-type and P/Q type components (Plummer *et al*., 1989; Regan *et al*., 1991; Mintz *et al*., 1992). Thus, the major types of neuronal high threshold Ca^{2+} channels in peripheral neurones are largely insensitive to 4030W92. In contrast, more marked inhibitory effects on the transient T-type current (Fox *et al*., 1987) were observed with 42% inhibition at 100 μM 4030W92. This is perhaps unsurprising given the effect of 4030W92 on inactivation states of Na^+ channels and the similarities, especially in terms of inactivation, between the atypical voltage-gated Ca^{2+} channels conducting T-type current and Na^+ channels (see Ertel & Ertel, 1997).

An important part of the present study was the profile of inhibition by 4030W92 of trains of action potentials observed in the current clamp experiments. The predominant effect of 4030W92 was to attenuate the later spikes in a train by apparently facilitating action potential accommodation. Close scrutiny of the initial period following current injection revealed that 4030W92 produced only modest inhibition of the first action potential. This characteristic is consistent with the voltage- and use-dependent inhibition of Na^+ channels observed under voltage-clamp. As the membrane is depolarized Na^+ channels are first opened and then inactivated. 4030W92 slows recovery from inactivation and thus reduces channel availability for subsequent Na^+ spikes. The cumulative reduction in Na^+ channel availability on repeated gating eventually results in insufficient Na^+ conductance to generate an action potential, and hence an abbreviation in the train of spikes. Of course, any direct reduction in membrane Ca^{2+} conductance, through T-type channels by 4030W92, may add to this effect, since low-voltage-activated Ca^{2+} channels may serve a role in triggering repetitive firing of neurones (see Ertel & Ertel, 1997 for review).

Can the state-dependent inhibitory effects of 4030W92 on voltage-gated Na^+ channels in sensory neurones be rationalized in terms of the antihyperalgesic profile of this agent *in vivo*? It is well established that agents such as prostaglandin E_2 and 5-HT that are released at a site of tissue injury lower the threshold of nociceptors by initiating a cascade of events that results in a change in ionic conductances at the nociceptor nerve terminal (England *et al*., 1996; Gold *et al*., 1996a; Cardenas *et al*., 1997). For PGE_2 a key step in this process following receptor activation is proposed to be a adenosine 3′ : 5′-cyclic monophosphate dependent (cyclic AMP) protein kinase-mediated phosphorylation of TTX_R. This channel phosphorylation results in an increase in current amplitude, a hyperpolarizing shift in the conductance-voltage relationship and acceleration of current activation and inactivation. Thus, TTX_R may be a critical determinant of nociceptor excitability under conditions of tissue injury or inflammation (England *et al*., 1996; Gold *et al*., 1996b). One possibility, therefore, is that inhibition of TTX_R by 4030W92 reduces the sensitization of nociceptors thereby preventing hyperalgesia.

In neuropathic pain states inhibitory effects of 4030W92 on TTX_S may become more important. For example, after axotomy of the sciatic nerve in the rat the amplitude of TTX_R in C-type DRG neurones was significantly reduced (Rizzo *et al*., 1995; Cummins & Waxman, 1997) and in parallel, the mRNA for the TTX_R channel-encoding sensory-neurone specific α-subunit was downregulated (Waxman *et al*., 1994; Dib-Hajj *et al*., 1996). However, in the same experiments, brain type III Na^+ channel mRNA was markedly elevated and an accompanying increase in the fast, TTX_S current was observed (Waxman *et al*., 1994; Dib-Hajj *et al*., 1996; Cummins & Waxman, 1997). These changes in the Na^+ channel density may underlie the initiation of ectopic discharges from the neuroma and the abnormal somatodendritic hyperexcitability of axotomized neurones (Devor *et al*., 1993; Matzner & Dever, 1994; Waxman *et al*., 1994; Cummins & Waxman, 1997). Thus, the efficacy of 4030W92 in animal models of neuropathic pain (Collins *et al*., 1998) may stem from Na^+ channel block at the neuroma thereby attenuating the high frequency firing of damaged peripheral neurones.

In both scenarios the voltage- and use-dependent nature of the effects of 4030W92 on Na^+ channels would predispose neurones which are depolarized and/or rapidly firing, to inhibition. On repeated intense stimulation of sensory neurones slow-inactivation states of Na^+ channels may accumulate and thus become susceptible to drug binding. In contrast, under normal conditions the effects of 4030W92 would be weak since prolonged depolarization and accumulation of Na^+ channels in the slow inactivated state would be minimal. Indeed, this may provide the basis for the 'antihyperalgesic' action of 4030W92, whereby the transmission of 'normal' physiological nociceptive information (e.g. 'pin-prick' pain) is spared by the drug, but the hyperalgesia resulting from inflammation or neuronal injury is attenuated (Clayton *et al*., 1998).

In summary, 4030W92 is a new, voltage- and use-dependent Na^+ channel inhibitor that enhances spike frequency adaptation in rat sensory neurones. This profile can be explained by a selective action of the drug on a slow

inactivation channel state. The state-dependent modulation of Na^+ channels, that are important in the function of sensory neurones, by 4030W92 may contribute to the antihyperalgesic properties of this compound.

The authors wish to thank Dr Malcolm Nobbs (Medicinal Sciences, Glaxo-Wellcome) for his helpful advice and comments.

References

AKOPIAN, A.N., SIVILOTTI, L. & WOOD, J.N. (1996). A tetrodotoxin-resistant sodium channel expressed by sensory neurones. *Nature,* **379,** 257–262.

BACK, F.W., JENSEN, T.S., KASTRUP, J., STIGSBY, B. & DEJGARD, A. (1990). The effect of intravenous lidocaine on nociceptive processing in diabetic neuropathy. *Pain,* **40,** 29–34.

BLACK, J.A., DIB-HAJJ, S., MCNABOLA, K., JESTE, S., RIZZO, M.A., KOCSIS, J.D. & WAXMAN, S.G. (1996). Spinal sensory neurones express multiple sodium channel α-subunit mRNAs. *Mol. Brain Res.,* **43,** 117–131.

BLACK, J.A. & WAXMAN, S.G. (1996). Sodium channel expression: a dynamic process in neurones and non-neuronal cells. *Dev. Neurosci.,* **18,** 139–152.

BOAS, R.A., COVINO, B.G. & SHAHNARIAN, A. (1982). Analgesic responses to i.v. lignocaine. *Br. J. Anaesthesiol.,* **54,** 501–505.

BOSSU, J.-L. & FELTZ, A. (1984). Patch-clamp study of the tetrodotoxin-resistant sodium current in group C sensory neurones. *Neurosci. Lett.,* **51,** 241–246.

CAFFREY, J.M., ENG, D.L., BLACK, J.A., WAXMAN, S.G. & KOCSIS, J.D. (1992). Three types of sodium channels in adult dorsal root ganglion neurones. *Brain Res.,* **592,** 283–297.

CARDENAS, C.G., DEL MAR, L.P., COOPER, B.Y. & SCROGGS, R.S. (1997). 5-HT_4 receptors couple positively to tetrodotoxin-insensitive sodium channels in a subpopulation of capsaicin-sensitive rat sensory neurones. *J. Neurosci.,* **17,** 7181–7189.

CARDENAS, C.G., DEL MAR, L.P. & SCROGGS, R.S. (1995). Variation in serotinergic inhibition of calcium currents in four types of rat sensory neurones differentiated by membrane properties. *J. Neurophysiol.,* **74,** 1870–1879.

CATTERAL, W.A. (1992). Cellular and molecular biology of voltage-gated sodium channels. *Physiol. Rev.,* **72,** S15–S48.

CHABAL, C., JACOBSEN, L., MARIANO, A., CHANEY, E. & BRITELL, C.W. (1992). The use of oral mexilitine for the treatment of pain after peripheral nerve injury. *Anaesthesiology,* **76,** 513–516.

CLAYTON, N.M., COLLINS, S.D., SARGENT, R., BROWN, T., NOBBS, M. & BOUNTRA, C. (1998). The effect of the novel sodium channel blocker 4030W92 in models of acute and chronic inflammatory pain in the rat. *Br. J. Pharmacol., Proc. Suppl.,* (in press).

COLLINS, S.D., CLAYTON, N.M., NOBBS, M. & BOUNTRA, C. (1998). The effect of 4030W92, a novel sodium channel blocker, on the treatment of neuropathic pain in the rat. *Br. J. Pharmacol., Proc. Suppl.* (in press).

CUMMINS, T.R. & WAXMAN, S.G. (1997). Downregulation of tetrodotoxin-resistant sodium currents and upregulation of a rapidly repriming tetrodotoxin-sensitive sodium current in small spinal sensory neurones after nerve injury. *J. Neurosci.,* **17,** 3503–3514.

DEJGARD, A., PETERSON, P. & KASTRUP, J. (1988). Mexilitine for treatment of chronic painful diabetic neuropathy. *Lancet,* **29,** 9–11.

DEVOR, M., GOVRIN-LIPPMAN, R. & ANGELIDES, K. (1993). Na^+ channel immunolocalisation in peripheral mammalian axons and changes following nerve injury and neuroma formation. *J. Neurosci.,* **13,** 1976–1992.

DIB-HAJJ, S., BLACK, J.A., FELTS, P. & WAXMAN, S.G. (1996). Down regulation of transcripts for Na channel subunit α-SNS in spinal sensory neurones following axotomy. *Proc. Natl. Acad. Sci. U.S.A.,* **93,** 14950–14954.

ELLIOTT, A.A. & ELLIOTT, J.R. (1993). Characterisation of TTX-sensitive and TTX-resistant sodium currents in small cells from adult rat dorsal root ganglia. *J. Physiol.,* **463,** 39–56.

ENGLAND, S., BEVAN, S. & DOCHERTY, R.J. (1996). PGE_2 modulates the tetrodotoxin-resistant sodium current in neonatal rat dorsal root ganglion neurones via the cyclic AMP-protein kinase A cascade. *J. Physiol.,* **495,** 429–440.

ERTEL, S.I. & ERTEL, E.A. (1997). Low voltage-activated T-type Ca^{2+} channels. *Trends Pharmacol. Sci.,* **18,** 37–42.

FOX, A.P., NOWYCKY, M.C. & TSIEN, R.W. (1987). Kinetic and pharmacological properties distinguishing three types of calcium currents in chick sensory neurones. *J. Physiol.,* **394,** 149–172.

GOLD, M.S., DASTMALCHI, S. & LEVINE, J.D. (1996a). Co-expression of nociceptor properties in dorsal root ganglion neurones from the adult rat *in vitro*. *Neuroscience,* **71,** 265–275.

GOLD, M.S., REICHLING, D.B., SHUSTER, M.J. & LEVINE, J.D. (1996b). Hyperalgesic agents increase a tetrodotoxin-resistant Na^+ current in nociceptors. *Proc. Natl. Acad. Sci. U.S.A.,* **93,** 1108–1112.

HAMILL, O.P., MARTY, A., NEHER, E., SAKMANN, B. & SIGWORTH, F.J. (1981). Improved patch clamp techniques for high-resolution current recording from cells and cell-free membrane patches. *Pflügers Arch.,* **391,** 85–100.

HERBERT, T., DRAPEAU, P., PRADIER, L. & DUNN, R.J. (1994). Block of the rat brain type IIA Na^+ channel α subunit by the neuroprotective drug riluzole. *Mol. Pharmacol.,* **45,** 1055–1060.

HILLE, B. (1993). Mechanisms of block. In: *Ionic channels of excitable membranes*. ed Hille, B. Ch. 15 pp. 390–422. Massachusetts: Sinauer Associates Inc.

HODGKIN, A.L. & HUXLEY, A.F. (1952a). Currents carried by sodium and potassium ions through the membrane of the giant axon of Loligo. *J. Physiol.,* **116,** 449–472.

HODGKIN, A.L. & HUXLEY, A.F. (1952b). The components of membrane conductance in the giant axon of Loligo. *J. Physiol.,* **116,** 473–496.

KUO, C.-G. & BEAN, B.P. (1994). Slow binding of phenytoin to inactivated sodium channels in rat hippocampal neurones. *Mol. Pharmacol.,* **46,** 716–725.

MARCHETTINI, P., LACARENZA, M., MARANGONI, C., PELLEGATA, G., SOTGIU, M.L. & MIRNE, S. (1992). Lidocaine test in neuralgia. *Pain,* **48,** 377–382.

MATZNER, L. & DEVOR, M. (1994). Hyperexcitability at sites of nerve injury depends on voltage-sensitive Na^+ channels. *J. Neurophysiol.,* **72,** 349–359.

MINTZ, I.M., ADAMS, M.E. & BEAN, B.P. (1992). P-type calcium channels in rat central and peripheral neurones. *Neuron,* **9,** 85–95.

NAKAMURA-CRAIG, M. & FOLLENFANT, R.L. (1995). Effect of lamotrigine in the acute and chronic hyperalgesia induced by PGE_2 and in the chronic hyperalgesia in rats with streptozotocin-induced diabetes. *Pain,* **63,** 33–37.

OGATA, N. & TATEBAYASHI, H. (1992). Comparison of two types of Na^+ currents with low voltage-activated T-type Ca^{2+} current in newborn rat dorsal root ganglia. *Pflügers Arch.,* **420,** 590–594.

PLUMMER, M.R., LOTOTHETIS, D.E. & HESS, P. (1989). Elementary properties and pharmacological sensitivities of calcium channels in mammalian peripheral neurones. *Neuron,* **2,** 1453–1463.

RAGSDALE, D.S., SCHEUR, T. & CATTERALL, W.A. (1991). Frequency and voltage-dependent inhibition of type IIA Na^+ channels, expressed in a mammalian cell line, by local anaesthetic, anti-arrhythmic and anticonvulsant drugs. *Mol. Pharmacol.,* **40,** 756–765.

REGAN, L.J., SAH, D.W.Y. & BEAN, B.P. (1991). Ca^{2+} channels in rat central and peripheral neurones: high threshold current resistant to dihydropyridine blockers and ω-conotoxin. *Neuron,* **6,** 269–280.

RIZZO, M.A., KOCSIS, J.D. & WAXMAN, S.G. (1995). Selective loss of slow and enhancement of fast Na^+ currents in cutaneous afferent dorsal root ganglion neurones following axotomy. *Neurobiol. Dis.,* **2,** 87–96.

ROY, M.L. & NARAHASHI, T. (1992). Differential properties of tetrodotoxin-sensitive and tetrodotoxin-resistant sodium channels in rat dorsal root ganglion neurones. *J. Neurosci.,* **12,** 2104–2111.

RUSH, A.M. & ELLIOTT, J.R. (1997). Phenytoin and carbamazepine: differential inhibition of sodium currents in small cells from adult rat dorsal root ganglia. *Neurosci. Lett.,* **226,** 905–998.

SANGAMESWARAN, L., DELGADO, S.G., FISH, L.M., KOCH, B.D., JAKEMAN, L.B., STEWART, G.R., SZE, P., HUNTER, J.C., EGLEN, R.M. & HERMAN, R.C. (1996). Structure and function of a noval voltage-gated tetrodotoxin-resistant sodium channel specific to sensory neurones. *J. Biol. Chem.,* **271,** 5953–5956.

SONG, J.-H., HUANG, C.-S., NAGATA, K., YEH, J.Z. & NARAHASHI, T. (1997). Differential action of riluzole on tetrodotoxin-sensitive and tetrodotoxin-resistant Na^+ channels. *J. Pharmacol. Exp. Ther.,* **282,** 707–714.

SONG, J.-H., NAGATA, K., HUANG, C.-S., YEH, J.Z. & NARAHASHI, T. (1996). Differential block of two types of sodium channels by anticonvulsants. *Neuro Report,* **7,** 3031–3036.

SUNAMI, A., FAN, Z., SAWANOBORI, T. & HIRAOKA, M. (1993). Use-dependent block of Na^+ currents by mexiletine at the single channel level in guinea-pig ventricular myocytes. *Br. J. Pharmacol.,* **110,** 183–192.

TANELIAN, D.L. & BROSE, W.G. (1991). Neuropathic pain can be relieved by drugs that are use-dependent Na^+ channel blockers: lidocaine, carbamazepine and mexilitine. *Anaesthesiology,* **74,** 949–951.

TREZISE, D.J., JOHN, V.H., NOBBS, M.N. & XIE, X. (1998). Voltage- and use-dependent inhibition of voltage-gated Na^+ channels in rat sensory neurones by the novel antihypersensitivity agent, 4030W92. *Br. J. Pharmacol. Proc. Suppl.,* (in press).

WAXMAN, S.G., KOCSIS, J.D. & BLACK, J.A. (1994). Type III sodium channel mRNA is expressed in embryonic but not adult spinal sensory neurones, and is re-expressed following axotomy. *J. Neurophysiol.,* **72,** 466–470.

XIE, X.M. & GARTHWAITE, J. (1996). State-dependent inhibition of Na^+ currents by the neuroprotective agent 619C89 in rat hippocampal neurones and in a mammalian cell line expressing rat brain type IIA Na^+ channels. *Neuroscience,* **73,** 951–962.

XIE, X., LANCASTER, B., PEAKMAN, T. & GARTHWAITE, J. (1995). Interaction of the antiepileptic drug lamotrigine with recombinant rat brain type IIA Na^+ channels and with native Na^+ channels in rat hippocampal neurones. *Pflügers Arch.,* **430,** 437–446.

ZAKRZEWSKA, J.M., CHAUDRY, Z., NURMIKKO, T.J., PATTON, D.W. & MULLENS, E.L. (1997). Lamotrigine (Lamictal) in refractory trigeminal neuralgia: results from a double-blind placebo controlled crossover trial. *Pain,* **73,** 223–230.

(Received January 12, 1998
Revised March 4, 1998
Accepted March 31, 1998)